CPA-free amplification of sub-10-ps pulses in Ho:YLF to the mJ-level at 2-µm wavelength

Hinkelmann, Moritz, Schulz, Bastian, Wandt, Dieter, Morgner, Uwe, Frede, Maik, et al.

Moritz Hinkelmann, Bastian Schulz, Dieter Wandt, Uwe Morgner, Maik Frede, Jörg Neumann, Dietmar Kracht, "CPA-free amplification of sub-10-ps pulses in Ho:YLF to the mJ-level at 2-µm wavelength," Proc. SPIE 10896, Solid State Lasers XXVIII: Technology and Devices, 108960Q (7 March 2019); doi: 10.1117/12.2508378

SPIE.

Event: SPIE LASE, 2019, San Francisco, California, United States

CPA-free amplification of sub-10 ps pulses in Ho:YLF to the mJ-level at 2 µm wavelength

Moritz Hinkelmann[a], Bastian Schulz[b], Dieter Wandt[a], Uwe Morgner[a,c], Maik Frede[b], Jörg Neumann[a], and Dietmar Kracht[a]

[a]Laser Zentrum Hannover e.V., Laser Development Department, Ultrafast Photonics Group, Hollerithallee 8, D-30419 Hannover, Germany
[b]neoLase GmbH, Hollerithallee 17, D-30419 Hannover, Germany
[c]Institut für Quantenoptik, Leibniz Universität Hannover, Welfengarten 1, D-30167 Hannover, Germany

ABSTRACT

The generation of sub-10 ps pulses around a wavelength of 2 µm with pulse energy at millijoule-level in a compact CPA-free amplifier chain is presented. This laser source covers a broad range of pulse repetition frequencies from 1 to 100 kHz with a pulse peak power from 136 to 17 MW, respectively. We used highly doped Ho:YLF crystals to achieve an overall amplification factor of almost 52 dB. A characterization of these crystals regarding upconversion losses and attainable small-signal gain supports this work.

Keywords: Laser amplifiers, Infrared and far-infrared lasers

1. INTRODUCTION

The generation of intense laser pulses at a wavelength around 2 µm is of great importance for a multitude of applications including material processing, micromachining, metrology,[1] but also for pumping of optical parametric conversion stages for mid-IR generation.[2–5] Most commonly, the corresponding laser sources rely on two different approaches: frequency down-conversion driven by near-IR pump sources or the emission in thulium (Tm)- and holmium (Ho)-doped materials. The direct laser emission and amplification at 2 µm in Tm- and Ho-doped materials benefits from simple architectures and amplification schemes as well as from a comparably higher optical-to-optical efficiency. In recent years, Ho-doped crystals have proven to be suited for the generation of sub-10 ps pulses with pulse energies up to tens of millijoules. Chirped pulse amplification (CPA) in regenerative amplifiers (RA) is the most widely used amplification scheme. The first demonstration of millijoule-level picosecond pulses by Dergachev et al. in 2013 was based on a RA and subsequent single-pass amplification.[6] Pulse energies up to 11 mJ at a pulse repetition frequency (PRF) of 1 kHz have been achieved, however, with pulse durations in the range of 300 ps. In 2016, Grafenstein et al. presented a 2 µm CPA source, which generated 2-µm pulses with an energy of 55 mJ at 1 kHz repetition rate.[7] After temporal compression to a pulse duration of 4.3 ps the pulse energy was 25 mJ corresponding to a peak power of 4.4 GW. However, the PRF in Pockels cell-driven RAs is usually limited to the 1-10 kHz regime. In addition, the CPA scheme requires highly efficient pulse stretchers and compressors. In particular, the proper pulse compression in either grating-based compressors or chirped volume Bragg gratings can be challenging and costly. In contrast, we have shown a CPA-free multipass amplification approach in Ho-doped $YLiF_4$ (Ho:YLF) crystals just recently.[8] We achieved more than 140 µJ in a PRF-tunable design maintaining ultrashort pulse durations of about 8 ps and less, depending on the PRF. Nevertheless, some strong-field applications demand for intense laser pulses, thus, millijoule-level pulse energies. A compact CPA-free laser source, capable of generating such pulse energies even at PRFs exceeding 10 kHz, is a versatile tool in a broad field of applications, but its development is still pending. In a CPA-free amplifier approach, short crystal lengths and high doping concentrations in combination

Further author information: (Send correspondence to M.H.)
M.H.: E-mail: m.hinkelmann@lzh.de
B.S.: E-mail: bs@neolase.com

Solid State Lasers XXVIII: Technology and Devices, edited by W. Andrew Clarkson, Ramesh K. Shori, Proc. of SPIE
Vol. 10896, 108960Q · © 2019 SPIE · CCC code: 0277-786X/19/$18 · doi: 10.1117/12.2508378

with proper beam diameters are necessary to keep the nonlinear effects as low as possible and at the same time maintain a high gain factor. A special attention has to be focused on the laser-induced damage threshold of the gain material. Especially, the high peak power levels of the ultrashort pulses in the focus inside the gain medium demand for a carefully tailored beam size to preserve damage-free operation. Furthermore, Ho-doped materials suffer from upconversion effects, by which two closely located Ho atoms in the ${}^5I_7$ manifold interact to promote one of them to the ${}^5I_5$ and to demote the other to the ${}^5I_8$ manifold. This deleterious process sets an upper limit for the doping concentration in Ho-doped gain media.

In this contribution, we show mJ-level pulse energies from a CPA-free multipass amplifier based on highly doped Ho:YLF, which is in principle not limited by the PRF. Additionally, we describe the lifetime quenching in highly doped Ho:YLF crystals in dependence on the excitation intensity and the doping concentration.

2. HOLMIUM CRYSTAL CHARACTERIZATION

The upper-state lifetime τ_f is an important parameter for engineering lasers and amplifiers. It affects the achievable stored-energy and, as a consequence, the overall output efficiency of the laser. High doping concentrations and strongly focused pumping, which are essential for high gain ultrashort pulse amplifiers, result in high population inversion densities. This promotes energy-transfer upconversion losses in Ho-doped crystals, which negatively influence the laser operation. Experimentally, upconversion can be visualized by measuring the excited state fluorescence decay. It manifests itself in lifetime quenching and a nonexponential decay slope. Both the excitation intensity and the doping concentration influence the fluorescence decay as both contribute to the population inversion density. Hence, the upconversion process is most important, when the energy storage in the ${}^5I_7$ manifold of the Ho^{3+} ion is high.

In 2003, Barnes et al. published the investigation of Ho:Ho upconversion energy-transfer parameters in different host crystals including Ho-doped YLF.[9] However, the investigated doping concentrations started at rather high values of 1 % (even 2 % in the case of Ho:YLF) because of difficulties to determine values for low concentrations. In order to roughly estimate the possible impact to our laser system, we measured the excited state fluorescence lifetime of the transition ${}^5I_7 \rightarrow {}^5I_8$, which is shown in Fig. 1. We investigated different a-cut Ho-doped YLF crystals with doping concentrations between 0.5 and 1.5 at. %.

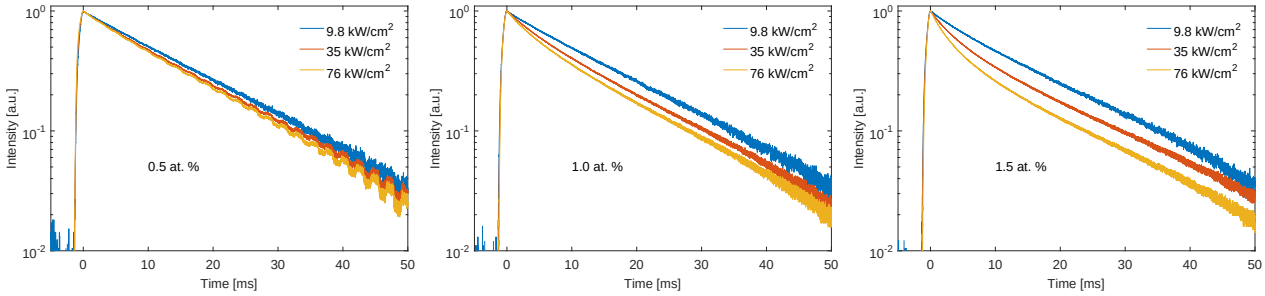

Figure 1. Normalized fluorescence decay curves in Ho:YLF at several pumping intensities.

In the case of 0.5 % doping concentration the decay is almost exponential and shows only a weak dependence in terms of the excitation intensity, whereas higher doping concentrations show a nonexponential form within the first 10 ms, in particular, at medium (35 kW/cm^2) and high (76 kW/cm^2) pump intensities. We calculated an upper-state lifetime τ_f by fitting an exponential decay to the time period between 0 and 5 ms. The results are summarized in Tab. 1. We have to note that an exponential fit is only valid for the rather weak excitation (9.8 kW/cm^2). However, fitting the nonexponential curves only within the first 5 ms approximates with the experimental data for a convincing comparison.

We measured an upper-state lifetime of 14.6 ms at low 0.5 at. % doping concentration and weak excitation intensity. This value agrees with literature data.[10,11] The lifetime of the ${}^5I_7$ population is then quenched to 12.1 ms, 8.4 ms, and 5.7 ms at high excitation intensity for doping concentrations of 0.5, 1.0, and 1.5 at. %, respectively. The effect of lifetime quenching in such lasers gets most prominent when pulse repetition frequencies

Table 1. Measured excited-state fluorescence lifetime of different Ho-doped YLF crystal samples.

Excitation intensity [kW/cm^2]	0.5 at. %	1.0 at. %	1.5 at. %
9.8	14.6 ms	13.6 ms	11.9 ms
35	12.8 ms	9.8 ms	7.6 ms
76	12.1 ms	8.4 ms	5.7 ms

close to or below the inverse of τ_f are applied. In this case, most of the stored energy is lost due to the upconversion process. As a first estimate, we believe that high doping concentrations up to 1.5 at. % can still be applied in kilohertz-rate laser systems.

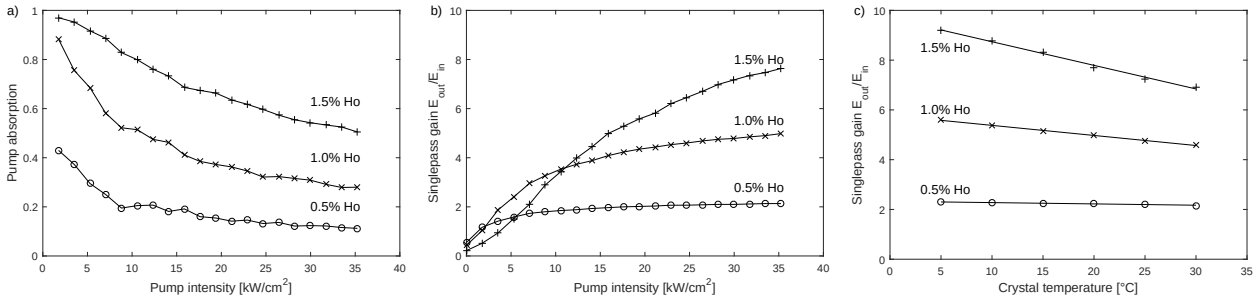

Figure 2. (a) 1940-nm continuous wave pump absorption, (b) single-pass small-signal gain, and (c) gain dependence on the temperature in Ho(0.5/1.0/1.5%):YLF.

The following investigation will show the capabilities of highly doped Ho:YLF crystals for such high PRFs. In a simple experiment we measured the small-signal single-pass gain of 4-ps pulses centered at 2051 nm in Ho:YLF with doping concentrations of 0.5, 1.0, and 1.5 at. %. Since the energy storage in this amplification regime is high, upconversion losses will be revealed. The crystal length is 20 mm and the beam waist radius is set to 85 µm. The signal pulse energy was 8.5 nJ at a PRF of 100 kHz. We used a maximum pump power of 4 W corresponding to a pump intensity of about 35 kW/cm^2 in the focal area inside the investigated crystals. In Figure 2a the 1940-nm pump absorption in dependence on the incident power for the different Ho:YLF samples is given. One can clearly see a bleaching of the crystals for high pump intensities, which can be attributed to the quasi-3-level energy scheme of the Ho^{3+} ion. In Figure 2b the single-pass gain with increasing pump power for different Ho:YLF samples is presented. At highest applied pump power level we achieved a gain factor of 2.1 (0.5 %), 5 (1.0 %), and 7.6 (1.5 %). At lower pump intensities of $<$ 5 kW/cm^2 ($<$ 10 kW/cm^2) the Ho(0.5 %):YLF (Ho(1.0 %):YLF) sample outperforms the higher doping concentrations. This can be explained by the strong absorption at high doping levels, and thus, an inhomogeneous distribution of the population inversion, which may result in rather low signal gain at the end of the crystal or even re-absorption. In addition, we investigated the gain dependence on the crystal temperature at highest pump intensity of 35 kW/cm^2. While the fitted slope (Figure 2c, black solid line) for 0.5 at. % is rather small with 0.5 %/K, it is significantly stronger for 1.5 at. % with 9.5 %/K. These results confirm that Ho doping concentrations as high as 1.5 at. % in YLF crystals can be applied for high repetition rate amplifiers. During all of the above experiments a clear luminescence of our Ho:YLF crystals in the visual spectrum indicated an higher-order upconversion mechanism.

3. EXPERIMENTAL SETUP

The laser system, as depicted in Fig. 3, consists of four major parts: (1) an all-fiber ultrashort seed source generating sub-10 ps in the spectral region of 2 µm,[12] (2) an acousto-optical modulator (AOM) for pulse-picking, (3) a 42-dB gain multipass amplifier based on a Ho(1.5 at. %):YLF crystal,[8] and (4) a single-pass booster amplifier in a dual-crystal design with a Ho(1.0 at. %):YLF crystal followed by a Ho(1.5 at. %):YLF crystal. The Ho:fiber-based seed source is generating up to about 70 nJ pulse energy at a fundamental PRF of 24 MHz.

The AOM exhibits about 50 % diffraction efficiency for the 2-µm radiation. The input pulse energy from the ultrashort pulse oscillator is set to 20 nJ taking into account the maximum input power of 500 mW as specified by the manufacturer. This results in a seed pulse spectral bandwidth of 1.7 nm at a central wavelength of 2051 nm. Considering the aforementioned diffraction efficiency of the AOM and losses of several optical components, about 10 nJ can be used as input for the crystal-based amplifiers. Measuring the autocorrelation revealed a seed pulse duration of about 5 ps. The high gain in the following multipass amplifier has been achieved by folding pump and signal beam such that they pass the Ho:YLF crystal six times with a focal beam diameter of 250 µm in the center of the crystal. The main amplifier is generating more than 100-µJ pulses maintaining sub-10 ps pulse duration. Finally, the single-pass dual-crystal amplifier boosts the pulse energy to the millijoule-level. The setup with two different doping concentrations is not only beneficial regarding the heat load distribution within the gain material, but also improves the homogeneity of the inverted fraction. The calculated pump absorption in this dual-crystal configuration is about 80 %. The beam diameter is significantly enlarged at 450 µm in order to mitigate laser-induced damage to the crystals. The Ho:YLF crystals exhibit a length of 20 mm and anti-reflection coating for the pump and the signal wavelength at 1940 nm and 2050 nm, respectively. They are wrapped in Indium foil and mounted in a copper heat sink, which is kept at about 20 °C.

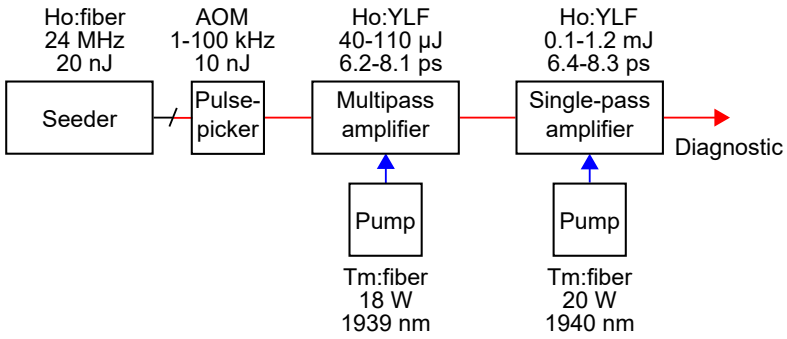

Figure 3. Schematic setup of the laser system. AOM: acousto-optical modulator.

For pumping, we use two Tm:fiber-based lasers with continuous emission at 1940 nm and an optical output power of about 20 W, each. Both pump sources are linearly polarized in order to meet the requirements of the uniaxial Ho:YLF crystals. The output wavelength has been tailored such that the narrow-band emission is located in between two distinct water absorption peaks, which are prevalent around 1940 nm. Pump and signal polarization are orientated along the crystallographic c-axis of all the Ho:YLF crystals. The whole amplifier chain fits on a breadboard with an area of about 1 m^2. It is working in ambient laboratory conditions without any effort made due to stability improvements.

4. EXPERIMENTAL RESULTS

Fig. 4 shows the multipass amplifier output pulse energy with increasing incident pump power for different PRFs ranging from 10 kHz up to 500 kHz. At pulse repetitions rates below about 50 kHz we were not able to exploit the complete pump power, since the amplifier started to lase in continuous wave operation on its own due to the high gain and comparably low seed power. At a repetition rate of 10 kHz we achieved up to 145 µJ pulse energy. The measured pulse duration was 8.3 ps corresponding to a pulse peak power of 16.4 MW. In Fig. 4 the stability of the multipass amplifier over a time period of more than 2 h is presented for a pulse energy of 44 µJ at 100 kHz. The root mean square noise amounts to less than 0.5 % confirming stable output. At the same time, this proves a good pointing stability since spatial instabilities would significantly affect the signal to pump beam mode matching. We did neither observe any thermal blooming of the pump beam due to the water absorption in the laboratory's environment nor any significant thermal lensing of the signal output beam. The optical-to-optical efficiency is between 15.5 % and 32 % at PRFs of 10 kHz and 500 kHz, respectively.

The second stage is a single-pass booster amplifier. As mentioned earlier, it consists of a sequential design of a Ho(1.0 at. %):YLF and a Ho(1.5 at. %):YLF crystal. Figure 5a shows the output pulse energy with increasing seed energy for different PRFs starting at 1 kHz up to 100 kHz. The incident pump power has been kept constant

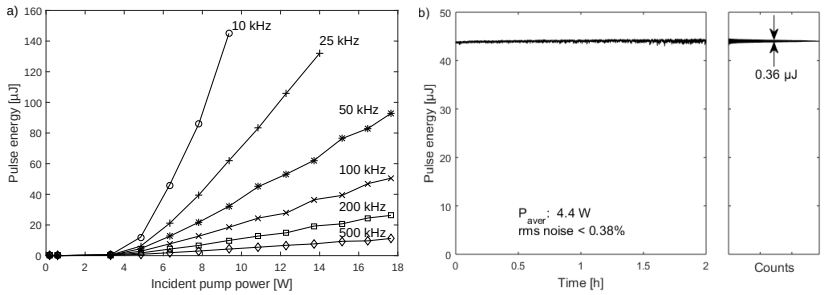

Figure 4. (a) Multipass amplifier output pulse energy versus pump power for different PRFs. (b) Long-term stability of the multipass amplifier at an average output power of 4.4 W at a PRF of 100 kHz.

at 18 W. The highest achieved pulse energy was 1.2 mJ at a PRF of 1 kHz. The single-pass gain of the booster amplifier was 11.9 in this case (see Figure 5b). The calculated maximum pulse fluence is about 1.5 J/cm^2. We believe that an even higher pulse energy will lead to laser-induced damage. In comparison, the highest achieved average output power was 10.6 W at a PRF of 100 kHz. This corresponds to an optical-to-optical power extraction efficiency of almost 40 % (see Figure 5b). In principle, energy scaling at the higher PRFs seems feasible. Here, we were only limited by the available pump power. Due to the quasi-3-level nature of the Ho^{3+} ions, cooling of the crystals to far below room temperature has the potential to further enhance the efficiency as described above. We measured the far-field beam profile (1.2 W at 1 kHz) with a scanning-slit beam profiler. The result is shown in Figure 5c and exhibits a rotationally symmetric Gaussian intensity distribution.

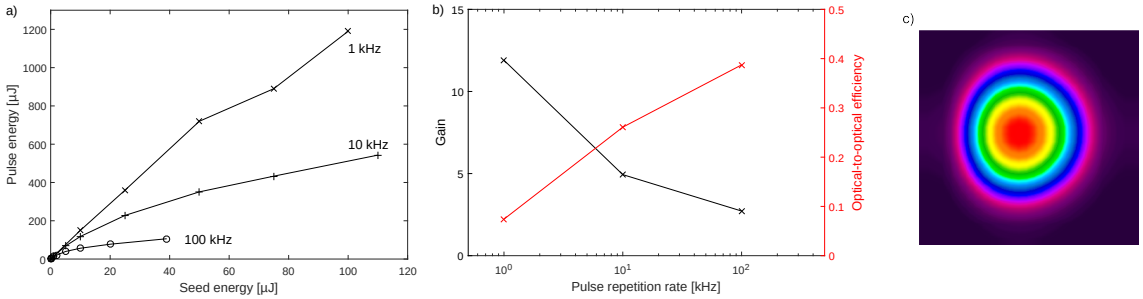

Figure 5. (a) Booster amplifier output pulse energy versus seed energy for different PRFs. (b) Single-pass gain of the booster stage and corresponding optical-to-optical efficiency. (c) Far-field beam profile measured with a scanning-slit beam profiler.

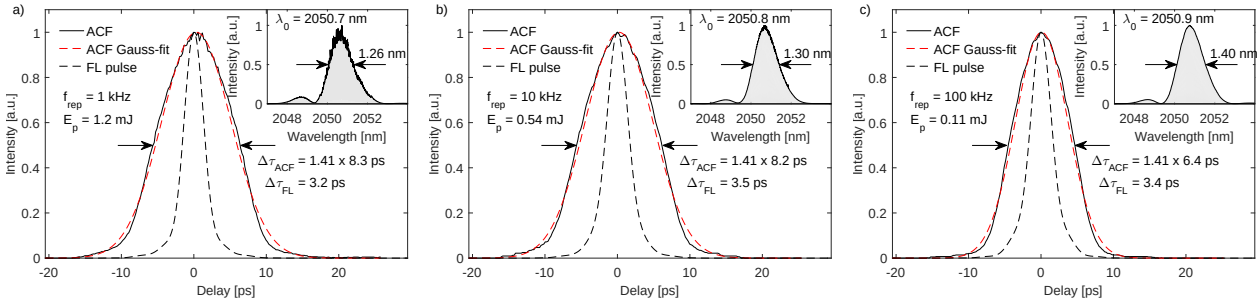

Figure 6. Autocorrelation traces at different pulse repetition rates (a) 1 kHz, (b) 10 kHz, and (c) 100 kHz. The dashed black line is the Fourier-limited pulse duration of the corresponding spectrum (inset).

The spectral and temporal characteristics for a PRF between 1 and 100 kHz are featured in Fig. 6a-c. The measured autocorrelation traces exhibit a sub-10 ps pulse duration over the full PRF tuning range. Taking into account the measured pulse energies, the corresponding pulse peak power is ranging from 136 to 17 MW at PRFs

of 1 to 100 kHz, respectively. Even at the highest pulse peak power we did not see any significant nonlinear effects or laser-induced damage of the crystal surface or bulk material. The calculated accumulated nonlinear phase, which is in the range of 1.4 rad, is below the critical value of π. The optical spectrum is centered around 2051 nm with a full-width at half-maximum of 1.26 nm (1 kHz), 1.3 nm (10 kHz), and 1.4 nm (100 kHz). The smaller bandwidth at lower pulse repetition rates can be explained by the gain narrowing effect due to the larger gain factor.

In principle, the generation of millijoule-level pulse energies at PRFs exceeding 1 kHz seems possible. Here, the pulse energy at repetition rates > 1 kHz is pump power-limited. High power Tm:fiber-based pump sources (> 100 W) are commercially available, but usually lack narrow-band emission in order to avoid atmospheric water absorption. For this reason, the development of such high repetition rate (> 10 kHz), millijoule-level laser sources might involve purging with dry air or nitrogen. We believe that cooling the crystal can further improve the gain factor, resulting in higher output pulse energies. This temperature dependency has been presented earlier in this manuscript.

5. CONCLUSION

In conclusion, we presented an ultrashort pulse laser system in the 2-µm spectral region with millijoule-level pulse energies. In combination with the rather simplified CPA-free amplification scheme and the PRF tunability, this laser source can be used for various applications. In addition, we investigated the impact of Ho:Ho upconversion for high energy amplifiers.

ACKNOWLEDGMENTS

German Federal Ministry of Education and Research (BMBF) (13N13974 NUKLEUS).

REFERENCES

[1] Scholle, K., Lamrini, S., Koopmann, P., and Fuhrberg, P., "2 µm laser sources and their possible applications," *in Frontiers in Guided Wave Optics and Optoelectronics, B. Pal, ed. (InTech, 2010)* , 471–500.

[2] Leindecker, N., Marandi, A., Byer, R. L., Vodopyanov, K. L., Jiang, J., Hartl, I., Fermann, M., and Schunemann, P. G., "Octave-spanning ultrafast opo with 2.6-6.1 µm instantaneous bandwidth pumped by femtosecond tm-fiber laser," *Optics Express* **20**(7), 7046–7053 (2012).

[3] Malevich, P., Andriukaitis, G., Flöry, T., Verhoef, A. J., Fernández, A., Ališauskasa, S., Pugžlys, A., Baltuška, A., Tan, L. H., Chua, C. F., and Phua, P. B., "High energy and average power femtosecond laser for driving mid-infrared optical parametric amplifiers," *Optics Letters* **38**(15), 2746–2749 (2013).

[4] Hemmer, M., Sánchez, D., Jelínek, M., Smirnova, V., Jelinkova, H., Kubeček, V., and Biegert, J., "2-µm wavelength, high-energy ho:ylf chirped-pulse amplifier for mid-infrared opcpa," *Optics Letters* **40**(4), 451–454 (2015).

[5] Sanchez, D., Hemmer, M., Baudisch, M., Cousin, S. L., Zawilski, K., Schunemann, P., Chalus, O., Simon-Boisson, C., and Biegert, J., "7 µm, ultrafast, sub-millijoule-level mid-infrared optical parametric chirped pulse amplifier pumped at 2 µm," *Optica* **3**(2), 147–150 (2016).

[6] Dergachev, A., "High-energy, kHz-rate, picosecond, 2-µm laser pump source for mid-IR nonlinear optical devices," in [*Solid State Lasers XXII: Technology and Devices*], *Proc. SPIE* **8599**, 85990B (2013).

[7] von Grafenstein, L., Bock, M., Ueberschaer, D., and Elsaesser, T., "Ho:YLF chirped pulse amplification at kilohertz repetition rates - 4.3 ps pulses at 2 µm with GW peak power," *Optics Letters* **41**(20), 4668–4671 (2016).

[8] Hinkelmann, M., Wandt, D., Morgner, U., Neumann, J., and Kracht, D., "High repetition rate, µJ-level, CPA-free ultrashort pulse multipass amplifier based on Ho:YLF," *Optics Express* **26**(14), 18125–18130 (2018).

[9] Barnes, N. P., Walsh, B. M., and Filer, E. D., "Ho:Ho upconversion: applications to Ho lasers," *Journal of the Optical Society of America B* **20**(6), 1212–1219 (2003).

[10] Payne, S. A., Chase, L. L., Smith, L. K., Kway, W. L., and Krupke, W. F., "Infrared Cross-Section Measurements for Crytslas Doped with Er^{3+}, Tm^{3+}, and Ho^{3+}," *IEEE Journal of Quantum Electronics* **28**(11), 2619–2630 (1992).

[11] Walsh, B. M., Barnes, N. P., and Bartolo, B. D., "Branching ratios, cross sections, and radiative lifetimes of rare earth ions in solids: Application to Tm^{3+} and Ho^{3+} ions in LiYF 4," *Journal of Applied Physics* **83**(5), 2772–2787 (1998).

[12] Hinkelmann, M., Wandt, D., Morgner, U., Neumann, J., and Kracht, D., "Mode-locked Ho-doped laser with subsequent diode-pumped amplifier in an all-fiber design operating at 2052 nm," *Optics Express* **25**(17), 4668–4671 (2017).